

Theoretical and Practical Aspects of Thermo Mechanical Reliability in Printed Circuit Boards with Copper Plated Through Holes

Stefan Neumann,
Nina Dambrowsky,
Stephen Kenny
Atotech Deutschland GmbH
Berlin, Germany

Abstract

The thermo mechanical reliability of copper plated through holes (PTH) in printed circuit boards is normally determined by different tests e.g. thermo cycle test (TCT), interconnect stress test (IST) or highly accelerated thermal shock (HATS).

During these tests the plated copper is exposed to stresses and strains which are below the tensile strength and the fracture strain, respectively, which leads to a strength-dependent fatigue failure mechanism.

To save time, as the duration of the above mentioned tests can vary between one day and several weeks, a knowledge of the functional relationship of the determining factors for the cycles to failure can be very helpful as it can provide the possibility to compute the dependency of the PTH copper reliability on different variables.

This paper introduces an extension to analytical considerations to estimate the influence of various parameters (e.g. coefficient of thermal expansion, temperature range, through hole diameter, thickness of PCB, thickness of plated copper) on the fatigue life of PTH copper during thermal excursion as published by Werner Engelmaier in [1]. The impact of in particular the glass transition temperature of the based material and also the final finish of the plated circuit board are also discussed.

The paper is completed with a discussion of the contribution of different parameters to the reliability of the through hole plated copper and the printed circuit board based on practical experience.

Introduction

Contemplating the fatigue life of metals which undergo cyclic mechanical stress the essential factor is the strain ε [1].

As the constituent parts of PCBs (e.g. epoxy, glass, copper, copper finish) show different thermo mechanical behaviour (e.g. different coefficients of thermal expansion α) each change of the temperature T results in thermo mechanical stresses/strains in the constituents. The relationship between the strain and the fatigue life can be expressed by so called Manson-Coffin plots. Figure 1 shows a Manson-Coffin plot of electrodeposited copper. It describes the influence of the strain (range) of the Cu on the (mean) cycles to failure. The higher the strain and the higher the portion of the plastic deformation the lower the fatigue life. An analysis of the Manson-Coffin plot of electrodeposited copper leads to the implicit equation ([1],[2])

$$N_f^{-0.6} D_f^{0.75} + 0.9 \frac{R_m}{E_{PTH Cu}} \left(\frac{e^{D_f}}{0.36} \right)^{0.1785 \log \left(\frac{10^5}{N_f} \right)} - \varepsilon = 0 \quad (1)$$

The first summand $N_f^{-0.6} D_f^{0.75}$ describes the influence of the plastic strain the second summand

$0.9 \frac{R_m}{E_{PTH Cu}} \left(\frac{e^{D_f}}{0.36} \right)^{0.1785 \log \left(\frac{10^5}{N_f} \right)}$ describes the influence of the elastic strain on the cyclic life where the meaning of the used parameters is as follows:

- N_f : expected fatigue life
- D_f : elongation at break, (fatigue) ductility
- R_m : tensile strength of PTH copper
- $E_{PTH Cu}$: modulus of elasticity of PTH copper, Young's modulus of PTH copper
- ε : total strain (elastic + plastic) of PTH copper

By modelling the thermo mechanical behaviour of a PCB the resulting strain ε (and stress) of the PTH copper becomes calculable. This allows to determine the expected fatigue life by solving equation (1).

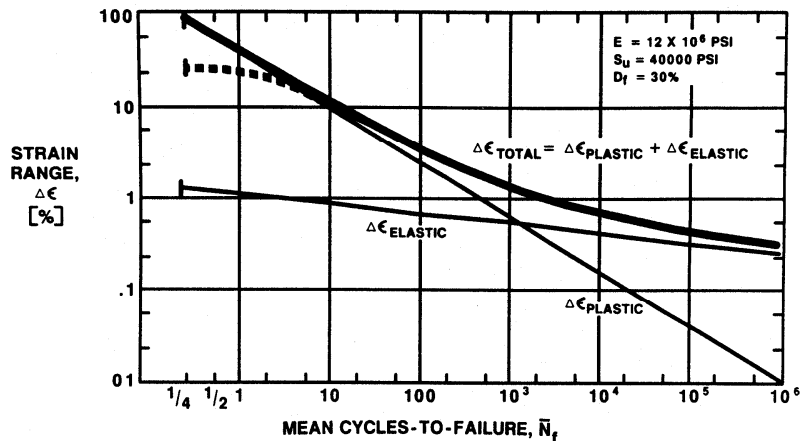


Figure 1: Manson-Coffin plot of electrodeposited copper [1].

1. Modelling the Thermo-mechanical Behaviour of a PCB

To model the thermo mechanical behaviour of a PCB several approximations and assumptions have to be made:

- Description of a PCB by analogy to a coupled spring system
- Introduction of “effective” areas
- Linearization of the PTH Cu stress-strain diagram
- Approximation of the glass transition
- Case differentiations

General assumptions

The following approximations and modeling include some general simplifying assumptions:

- No thermal variance of the Young's modulus
- No thermal variance of the PTH Cu ductility and the PTH Cu tensile strength
- Ideal drill holes: No roughness, no glass fiber protrusion, etc.
- Constant Young's modulus of the Cu finish (only elastic behavior considered)
- No inner layers
- No bending of the annular ring and perfect adhesion between base material and PTH Cu as well as between PTH Cu and Cu finish
- No variance of the PTH Cu thickness
- Gradient free distribution of temperature in the PCB

Description of a PCB by analogy to a spring system

To describe the behaviour of a PCB under thermo mechanical influence the different constituents are treated as springs which are coupled in such a way that the length of all springs are throughout equal. If the springs were loose a change of temperature would force different length changes subjected to the different coefficients of thermal expansion α of the springs. By coupling the springs the free elongation is suppressed and internal tensile/compressive stresses build up. Springs with a higher α are hindered in their expansion by springs with a lower α (\rightarrow compressive stress in spring with higher α) while springs with a lower α are extended by springs with a higher α (\rightarrow tensile stress in spring with lower α).

The system of coupled springs settles at a state of equilibrium of forces (compensation of expansive / compressive forces). At the state of equilibrium of forces all springs have the elongation ε_0 . The difference between ε_0 and the free expansion of the springs $\varepsilon_{i,free} = \alpha_i \Delta T$ (ΔT is the temperature difference) gives the strain in the particular spring. The strain of the “PTH Cu spring” then can be inserted into equation (1) to calculate the fatigue life of the PTH Cu.

Figure 2 shows sketches of coupled and non-coupled spring systems. The different constituents of the PCB are represented by different springs (Cu finish, PTH Cu, Epoxy). Figure 2a) depicts the spring system the start temperature. The coupled springs have an initial elongation $\varepsilon_{initial}$. In figure 2b) the behaviour of a system of non-coupled springs after a temperature increase is shown. Due to their

different coefficients of thermal expansion the springs show different (free) elongations. Figure 2c) shows the situation for the same temperature increase but with coupled springs. The system settles at a state of equilibrium with the elongation ϵ_0 .

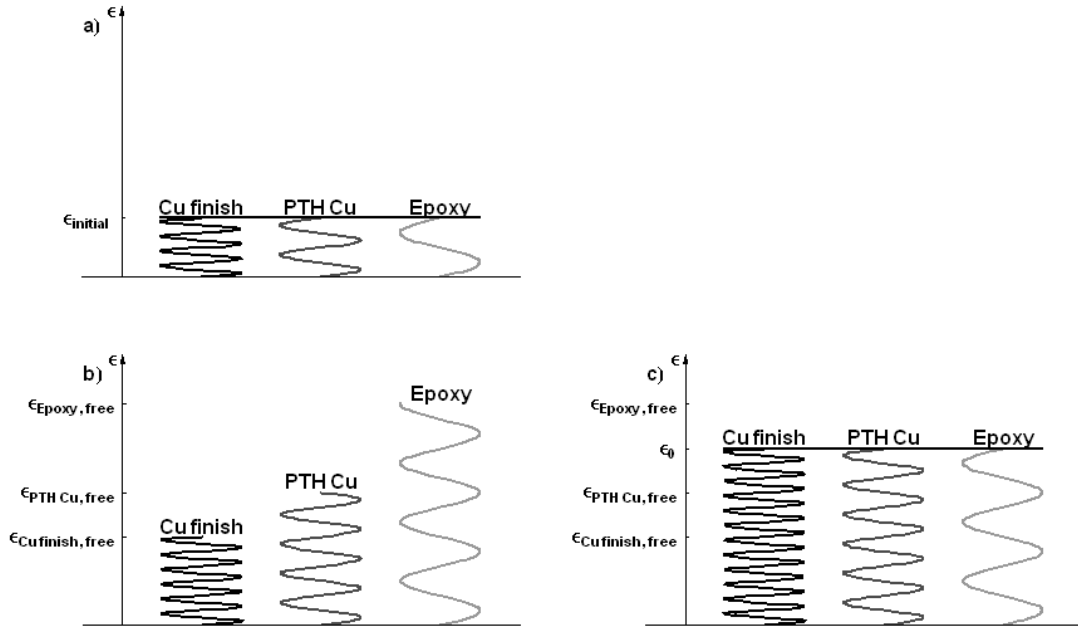


Figure 2: a) coupled spring system at start temperature, b) non-coupled spring system after temperature increase, c) coupled spring system after temperature increase

The relationship between the repulsing force F and the deflection ΔL of a linear mechanical spring is

$$F = -D\Delta L \quad (2)$$

where

D : spring constant

D is defined by

$$D = E \frac{A}{L_0} \quad (3)$$

where

E : Young's modulus of spring material

A : cross sectional area of spring

L_0 : initial length of spring

Inserted in expression (2) this leads to

$$F = -\frac{\Delta L}{L_0} EA = -\epsilon EA \quad (4)$$

In this model ϵ is the difference between the point of equilibrium of forces and the strain under free elongation (see fig. 2c).

As in this model the PCB consists of three components (base material (epoxy), PTH Cu, Cu finish) we get three force equations:

$$F_{\text{Epoxy}} = -\epsilon_{\text{Epoxy}} E_{\text{Epoxy}} A_{\text{Epoxy}} \quad (5)$$

$$F_{\text{PTH Cu}} = -\epsilon_{\text{PTH Cu}} E_{\text{PTH Cu}} A_{\text{PTH Cu}} \quad (6)$$

$$F_{\text{Cu finish}} = -\epsilon_{\text{Cu finish}} E_{\text{Cu finish}} A_{\text{Cu finish}} \quad (7)$$

where

$$\epsilon_{\text{Epoxy}} = \epsilon_0 - \epsilon_{\text{Epoxy, free}}$$

$$\epsilon_{\text{PTH Cu}} = \epsilon_0 - \epsilon_{\text{PTH Cu, free}}$$

$$\epsilon_{\text{Cu}} = \epsilon_0 - \epsilon_{\text{Cu finish, free}}$$

finish

An equilibrium of forces is reached if the sum of all forces F_{total} equals zero.

$$F_{\text{total}} = F_{\text{Epoxy}} + F_{\text{PTH Cu}} + F_{\text{Cu finish}} = 0 \quad (8)$$

Solving equation (8) for ε_0 and subtracting the free expansion $\varepsilon_{PTH\ Cu, free}$ then yields the strain $\varepsilon_{PTH\ Cu}$ of the PTH Cu.

“Effective” areas

The strain of the PTH copper is affected by different so called “effective” areas $A_{effective}$. The geometry of the constituents of the PCB influence the strain of the PTH copper. For example a thick PTH Cu barrel can withstand the driving force of the expanding base material better than a thin PTH Cu barrel. A parameter describing the amount of this influence is $A_{effective}$. The “influencing” areas of the different constituents are the cross sectional areas of the constituents which normal vectors are parallel to the tensile/compressive force direction. As the base material surrounds the PTH on a large scale the “influencing” area of the base material A_{Epoxy} has to be estimated by dimensional parameters of the PCB ([1],[3]).

$$A_{Epoxy} \cong \frac{\pi}{4} [(h + d)^2 - d^2] \quad (9)$$

with

h : thickness of base material

d : through hole diameter

The “influencing” area of the PTH Cu is its cross section.

$$A_{PTH\ Cu} = \frac{\pi}{4} [d^2 - (d - 2t_{PTH\ Cu})^2] \quad (10)$$

with

$t_{PTH\ Cu}$: thickness of PTH Cu

The “influencing” area of the Cu finish also is its cross section.

$$A_{Cu\ finish} = \pi t_{Cu\ finish} (d - t_{Cu\ finish} - 2t_{PTH\ Cu}) \quad (11)$$

with

t_{Cu} : thickness of Cu finish

^{finish}

Above mentioned variables are illustrated in figure 3 which shows a schematic of a PTH cross section.

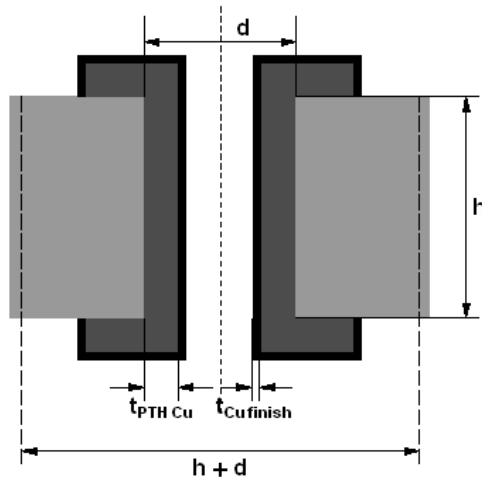


Figure 3: PTH cross section. Illustration of geometrical parameters.

Approximation of the stress-strain diagram of the PTH Cu

The stress-strain diagram gives the relationship between the tensile stress and the resulting elongation (strain) of a material (and vice versa). Usually materials show an elastic performance for stresses below the yield strength σ_y (Hooke’s law). In this region the slope of the stress-strain diagram

$$E_{el} = \frac{\Delta\sigma_{el}}{\Delta\varepsilon_{el}}$$

equals Young’s modulus

. For stresses above σ_y the behaviour of the stress-strain diagram is non-linear. To overcome the problems caused by handling non-linearity as a first approximation the plastic region of the stress-strain diagram is described by a linear branch which has the slope of the

$$E_{pl} = \frac{\Delta\sigma_{pl}}{\Delta\varepsilon_{pl}}$$

modulus of plasticity

In figure 4 a stress-strain diagram is depicted. It shows the elastic and plastic region and also the linearization of the plastic region (tangent line).

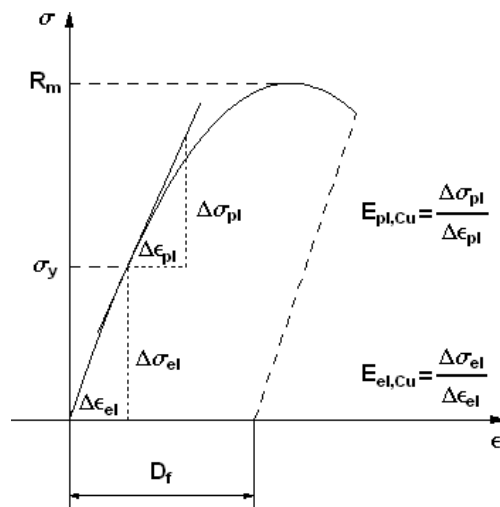


Figure 4: Stress-strain diagram of Cu. R_m : Tensile strength, D_f : Elongation at break (ductility)

Approximation of the coefficient of thermal expansion α and the glass transition temperature T_g

Standard PCB base materials (e.g. FR4) have a so called glass transition temperature which divides the material's properties into brittle (below T_g) and soft (above T_g) behaviour. While in the brittle "phase" the coefficient of thermal expansion (in z-direction) α is low (e.g. 50 ppm/K) and the modulus of elasticity E is high (e.g. 850 kN/cm²) in the soft "phase" α is significantly higher (e.g. 250 ppm/K) and E is significantly lower (e.g. 670 kN/cm²). A "real" glass transition is smooth but in this model it is handled as if it is punctual which results in a defined T_g with a linear branch below and above T_g . Figure 5 shows a sketch of a linearized glass transition diagram with a low α and high E for temperatures below T_g and a high α and low E for temperatures above T_g .

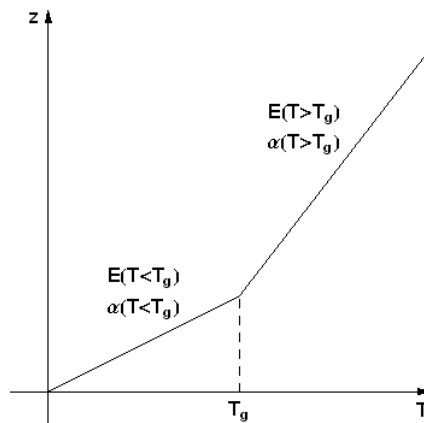


Figure 5: Linearized glass transition diagram.

Case differentiations

Due to the bilinearity of the stress strain relationship and the glass transition the parameters $E_{PTH\ Cu}$, α_{Epoxy} and E_{Epoxy} are constant only in sections. For example for stresses below the yield strength σ_y the Young's modulus of the PTH Cu has the constant value $E_{el, PTH\ Cu}$. Above σ_y the Young's modulus has the constant value $E_{pl, PTH\ Cu}$. In analogy the properties α_{Epoxy} and E_{Epoxy} have different (constant) values below and above the glass transitions temperature T_g .

Altogether this leads to five cases which have to be taken into account.

1.6.1 Case 1: Final temperature T_f below T_g and tensile stress at T_f $\sigma(T_f)$ below Cu yield strength σ_y

In this case the material properties do not change during cycling. By inserting the particular parameters (e.g. $E_{el,PTH\ Cu}$, $\alpha(T < T_g)$) and their values into the equations (5) to (7) equation (8) can be solved for ε_0 .

Figure 6 shows the linearized stress-strain-diagram of the PTH Cu at a final temperature T_f where the stress in the Cu $\sigma(T_f)$ is below the yield strength σ_y of the Cu.

Figure 7 shows the linearized glass transition diagram. At T_f the coefficient of thermal expansion has the value $\alpha(T < T_g)$ and the Young's modulus has the value $E(T < T_g)$.

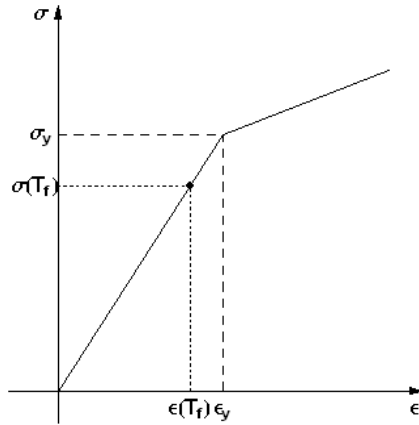


Figure 6: Linearized stress-strain-diagram of PTH copper. The tensile stress at the final temperature $\sigma(T_f)$ is below the yield strength σ_y .

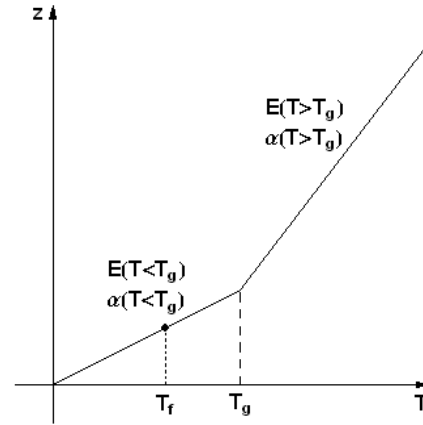


Figure 7: Linearized glass transition diagram. At the temperature T_f the coefficient of thermal expansion and the Young's modulus have the values $\alpha(T < T_g)$ and $E(T < T_g)$.

1.6.2 Case 2: Final temperature T_f below T_g and tensile stress at T_f $\sigma(T_f)$ above Cu yield strength σ_y

For final temperatures T_f below T_g the coefficient of thermal expansion and the modulus of elasticity of the base material stay constant but for mechanical stresses at T_f $\sigma(T_f)$ above the yield strength σ_y a changing of the Young's modulus of the PTH Cu has to be considered. Above σ_y the relation between the mechanical stress and the material elongation is described by the modulus of plasticity of the PTH Cu. In this case the formulation of the force in the PTH Cu is:

$$F_{PTH\ Cu} = -\varepsilon_y E_{el,PTH\ Cu} A_{PTH\ Cu} - (\varepsilon_0 - (\varepsilon_{PTH\ Cu, free} + \varepsilon_y)) E_{pl,PTH\ Cu} A_{PTH\ Cu} \quad (12)$$

The other force formulations are not affected.

Figure 8 shows the linearized stress-strain-diagram of the PTH Cu at a final temperature T_f where the stress in the Cu $\sigma(T_f)$ is above the yield strength σ_y of the Cu.

Figure 9 shows the linearized glass transition diagram. At T_f the coefficient of thermal expansion has the value $\alpha(T < T_g)$ and the Young's modulus has the value $E(T < T_g)$.

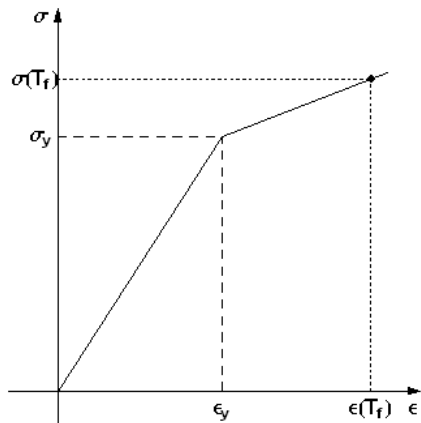


Figure 8: Linearized stress-strain-diagram of PTH. The tensile stress at the final temperature $\sigma(T_f)$ is above the yield strength σ_y .

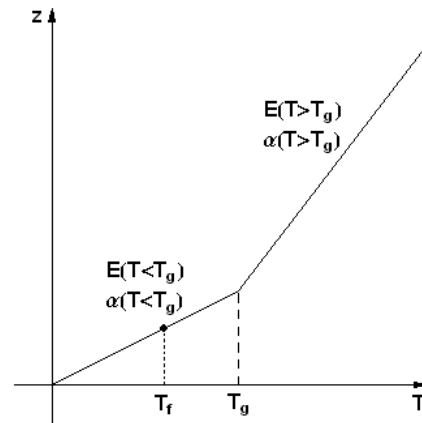


Figure 9: Linearized glass transition diagram. At the temperature T_f the coefficient of thermal expansion and the Young's modulus have the values $\alpha(T < T_g)$ and $E(T < T_g)$.

1.6.3 Case 3: Final temperature T_f above T_g , tensile stress at T_f $\sigma(T_f)$ and tensile stress at T_g $\sigma(T_g)$ below σ_y

For final temperatures T_f above T_g it has to be considered that the coefficient of thermal expansion and the modulus of elasticity of the base material change at T_g . The mechanical stress at T_f $\sigma(T_f)$ stays below the yield strength σ_y .

By dividing the temperature difference ΔT into two intervals ΔT_1 and ΔT_2 with

$$\Delta T_1 = T_g - T_s \quad (T_s \text{ start temperature})$$

$$\Delta T_2 = T_f - T_g$$

the elongation of the PTH Cu can be calculated by adding the elongations occurring at ΔT_1 and ΔT_2 . For the interval ΔT_1 the base material properties $E(T < T_g)$ and $\alpha(T < T_g)$ have to be chosen. For the interval ΔT_2 the base material properties $E(T > T_g)$ and $\alpha(T > T_g)$ have to be chosen.

Figure 10 depicts the linearized stress-strain-diagram of the PTH Cu at a final temperature T_f where the stress in the Cu $\sigma(T_f)$ is below the yield strength σ_y of the Cu but where T_f is above the glass transition temperature T_g of the base material. Figure 11 shows the linearized glass transition diagram. At T_f the coefficient of thermal expansion has the value $\alpha(T > T_g)$ and Young's modulus the value $E(T > T_g)$.

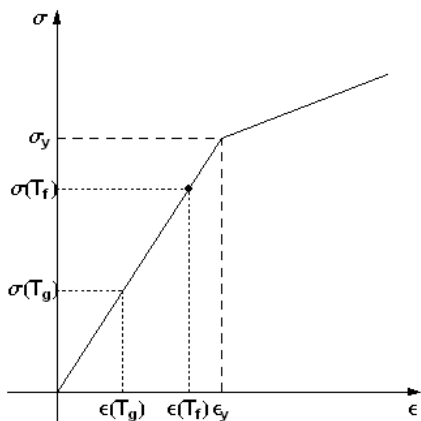


Figure 10: Linearized stress-strain-diagram of PTH. The tensile stress at the final temperature $\sigma(T_f)$ is below the yield strength σ_y .

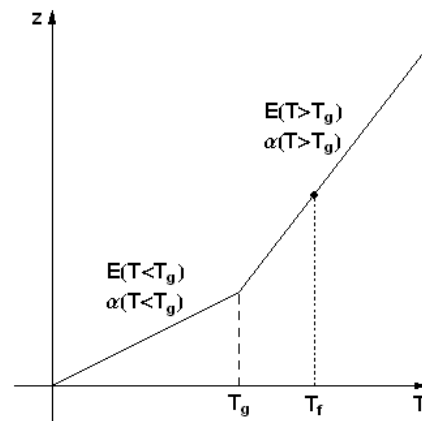


Figure 11: Linearized glass transition diagram. At the temperature T_f the coefficient of thermal expansion and the Young's modulus have the values $\alpha(T > T_g)$ and $E(T > T_g)$.

1.6.4 Case 4: Final temperature T_f above T_g , tensile stress at T_f $\sigma(T_f)$ above yield strength σ_y and tensile stress at T_g $\sigma(T_g)$ below σ_y

Similar to paragraph 1.6.3 the elongation of the PTH Cu can be calculated by subdividing the expansion into two steps. In the first step the strain until reaching the temperature T_g has to be calculated. Starting from this point the elongation between T_g and T_f has to be computed. To do so the yield strength σ_y has to be modified to

$$\sigma_y = \sigma_y - \sigma_g \quad (13)$$

Where σ_g is the stress in the PTH Cu at $T = T_g$.

Figure 12 shows the linearized stress-strain-diagram of the PTH Cu at a final temperature T_f where the stress in the Cu $\sigma(T_f)$ is above the yield strength σ_y of the Cu and where T_f is above the glass transition temperature T_g of the base material. At T_g the stress in the Cu is below σ_y . Figure 13 shows the linearized glass transition diagram. At T_f the coefficient of thermal expansion has the value $\alpha(T > T_g)$ and the Young's modulus the value $E(T > T_g)$.

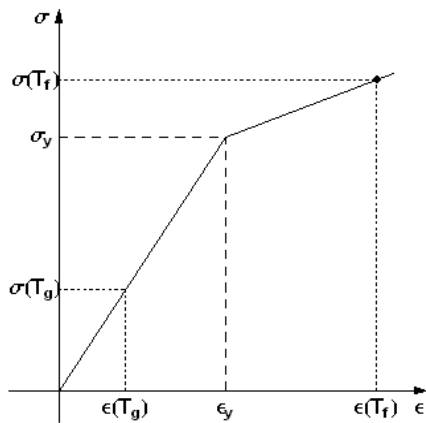


Figure 12: Linearized stress-strain-diagram of PTH. The tensile stress at the glass transition temperature $\sigma(T_g)$ is below the yield strength σ_y . The tensile stress at the final temperature $\sigma(T_f)$ is above the yield strength σ_y .

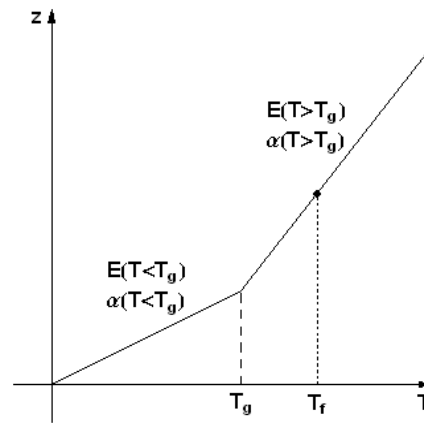


Figure 13: Linearized glass transition diagram. At the temperature T_f the coefficient of thermal expansion and the Young's modulus have the values $\alpha(T > T_g)$ and $E(T > T_g)$.

1.6.5 Case 5: Final temperature T_f above T_g , tensile stress at T_f $\sigma(T_f)$ above σ_y and tensile stress at T_g $\sigma(T_g)$ above σ_y

In analogy to 1.6.3 also here the elongation of the PTH Cu can be determined by subdividing the expansion into two steps. In the first step the expansion until reaching T_g has to be calculated (similar to case 2). In the second step the elongation between T_g and T_f has to be evaluated.

Figure 14 shows the linearized stress-strain-diagram of the PTH Cu at a final temperature T_f where the stress in the Cu $\sigma(T_f)$ is above the yield strength σ_y of the Cu and where T_f is above the glass transition temperature T_g of the base material. At T_g the stress in the Cu is above σ_y . Figure 15 shows the linearized glass transition diagram. At T_f the coefficient of thermal expansion has the value $\alpha(T > T_g)$ and Young's modulus the value $E(T > T_g)$.

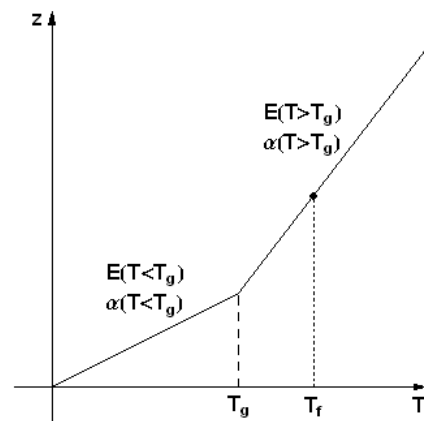
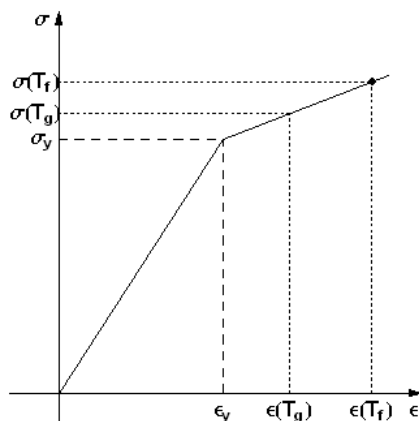


Figure 14: Linearized stress-strain-diagram of PTH copper. The tensile stress at the glass transition temperature $\sigma(T_g)$ and at the final temperature $\sigma(T_f)$ is above the yield strength σ_y .

Figure 15: Linearized glass transition diagram. At the temperature T_f the coefficient of thermal expansion and the Young's modulus have the values $\alpha(T > T_g)$ and $E(T > T_g)$.

2. Contribution of different parameters on the PTH reliability

Considering the case differentiations from chapter 1.6 an analysis of the dependency of the expected fatigue life N_f on changing different PCB parameters (e.g. PTH Cu thickness, CTE of base material, ductility of PTH Cu, diameter of drill hole, ...) can be made. Calculating the strain of the PTH Cu $\epsilon_{PTH\ Cu}$ and iteratively solving equation (1) yields N_f . To get "meaningful" results a knowledge of the material property parameters is needed. In many cases the equipment to measure these values is not available (e.g. young's modulus of base material, young's modulus of electroplated copper, etc.). To overcome this problem above mentioned values have to be assumed (e.g. material property data bases).

Investigation of the influence of the PTH Cu ductility D against the base material glass transition temperature T_g

To analyze the influence of the PTH Cu ductility D and the glass transition temperature T_g on the thermo mechanical reliability of a PCB D has been varied between 15% and 25% and T_g has been varied between 100°C and 150°C.

An overview of the used parameters and their values shows table 1.

Table 1: Parameters used to analyze the influence of D and T_g on N_f

T_s	25 °C	D	15 % – 25 %
T_f	150 °C	R_m	30 kN/cm ²
h	1.6 mm	$E_{Cu\ finish}$	-
d	300 μ m	$\alpha_{Cu\ finish}$	-
$t_{PTH\ Cu}$	25 μ m	T_g	100 °C – 150 °C
$t_{Cu\ finish}$	0 μ m	$E_{Epoxy}(T < T_g)$	848 kN/cm ²
$E_{el, PTH\ Cu}$	12400 kN/cm ²	$E_{Epoxy}(T > T_g)$	676 kN/cm ²
$E_{pl, PTH\ Cu}$	117 kN/cm ²	$\alpha_{Epoxy}(T < T_g)$	60 ppm/K
$\alpha_{PTH\ Cu}$	17 ppm/K	$\alpha_{Epoxy}(T > T_g)$	250 ppm/K
σ_y	25 kN/cm ²		

In figure 16 the effect of changing D and T_g on the reliability of PCBs is displayed. As can be seen the effect of changing the glass transition temperature T_g of the PCB base material dominates over the influence of changing the ductility of the PTH copper.

For example a ductility of 25% and a glass transition temperature of 130°C yield the same number of cycles as a ductility of 15% and a glass transition temperature of 140°C (see contour lines of figure 16).

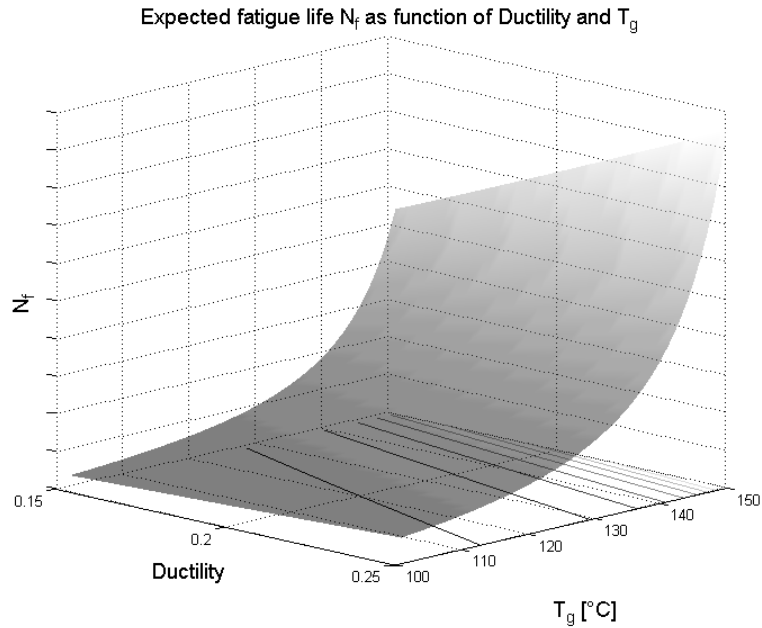


Figure 16: Number of stress cycles as function of D and T_g

Investigation of the influence of PTH Cu ductility D against the coefficient of thermal expansion of the base material below T_g $\alpha_{Epoxy}(T < T_g)$

To analyze the influence of the PTH Cu ductility D and the coefficient of thermal expansion of the base material below the glass transition temperature $\alpha_{Epoxy}(T < T_g)$ on the reliability of a PCB D has been varied between 15% and 25% and $\alpha_{Epoxy}(T < T_g)$ has been varied between 40 ppm/K and 60 ppm/K. An overview of the used parameters and their values shows table 2.

Table 2: Parameters used to analyze the influence of D and $\alpha_{Epoxy}(T < T_g)$ on N_f

T_s	25 °C	D	15 % – 25 %
T_f	150 °C	R_m	30 kN/cm ²
h	1.6 mm	$E_{Cu\ finish}$	-
d	300 μ m	$\alpha_{Cu\ finish}$	-
$t_{PTH\ Cu}$	25 μ m	T_g	145°C
$t_{Cu\ finish}$	0 μ m	$E_{Epoxy}(T < T_g)$	848 kN/cm ²
$E_{el, PTH\ Cu}$	12400 kN/cm ²	$E_{Epoxy}(T > T_g)$	676 kN/cm ²
$E_{pl, PTH\ Cu}$	117 kN/cm ²	$\alpha_{Epoxy}(T < T_g)$	40 ppm/K - 60 ppm/K
$\alpha_{PTH\ Cu}$	17 ppm/K	$\alpha_{Epoxy}(T > T_g)$	250 ppm/K
σ_y	25 kN/cm ²		

In figure 17 the effect of changing D and $\alpha_{Epoxy}(T < T_g)$ on the reliability of PCBs is displayed. As can be seen the effect of changing the coefficient of thermal expansion $\alpha_{Epoxy}(T < T_g)$ of the PCB base material dominates over the influence of changing the ductility of the PTH copper. For example a ductility of 25% and a coefficient of thermal expansion of ≈ 55 ppm/K yield the same number of cycles as a ductility of 15% and a coefficient of thermal expansion of ≈ 48 ppm/K (see contour lines of figure 17).

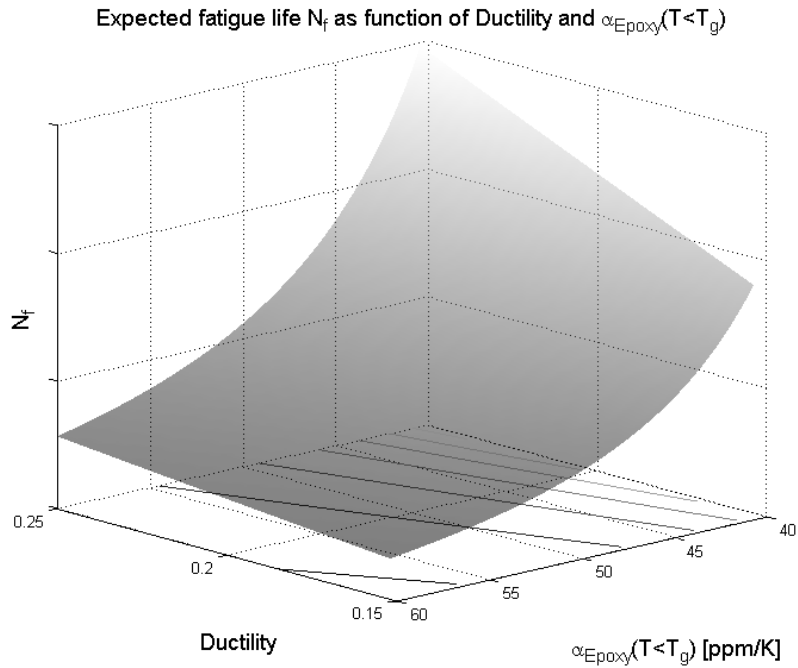


Figure 17: Number of stress cycles as function of D and $\alpha_{\text{Epoxy}}(T < T_g)$

Investigation of the influence of the Young's modulus $E_{\text{Cu finish}}$ and the coefficient of thermal expansion $\alpha_{\text{Cu finish}}$

To analyze the influence of the Cu finish on the reliability of a PCB the Young's modulus $E_{\text{Cu finish}}$ and the coefficient of thermal expansion $\alpha_{\text{Cu finish}}$ of the Cu finish has been varied. The PTH Cu thickness was set to 25 μm and the thickness of the PTH Cu finish was set to 5 μm . $E_{\text{Cu finish}}$ was chosen between 5000 kN/cm^2 and 20000 kN/cm^2 and $\alpha_{\text{Cu finish}}$ has been varied between 10 ppm/K and 30 ppm/K .

An overview of the used parameters and their values shows table 3.

Table 3: Parameters used to analyze the influence of $E_{\text{Cu finish}}$ and $\alpha_{\text{Cu finish}}$ on N_f

T_s	25 °C	D	20 %
T_f	150 °C	R_m	30 kN/cm^2
h	1.6 mm	$E_{\text{Cu finish}}$	5000 kN/cm^2 - 20000 kN/cm^2
d	300 μm	$\alpha_{\text{Cu finish}}$	10 ppm/K – 30 ppm/K
$t_{\text{PTH Cu}}$	25 μm	T_g	145°C
$t_{\text{Cu finish}}$	5 μm	$E_{\text{Epoxy}}(T < T_g)$	848 kN/cm^2
$E_{\text{el, PTH Cu}}$	12400 kN/cm^2	$E_{\text{Epoxy}}(T > T_g)$	676 kN/cm^2
$E_{\text{pl, PTH Cu}}$	117 kN/cm^2	$\alpha_{\text{Epoxy}}(T < T_g)$	55 ppm/K
$\alpha_{\text{PTH Cu}}$	17 ppm/K	$\alpha_{\text{Epoxy}}(T > T_g)$	270 ppm/K
σ_y	25 kN/cm^2		

In figure 18 the effect of changing $E_{\text{Cu finish}}$ and $\alpha_{\text{Cu finish}}$ on the reliability of PCBs is displayed.

Expected fatigue life N_f as function of the Cu finish Young's Modulus and $\alpha_{Cu\ finish}$

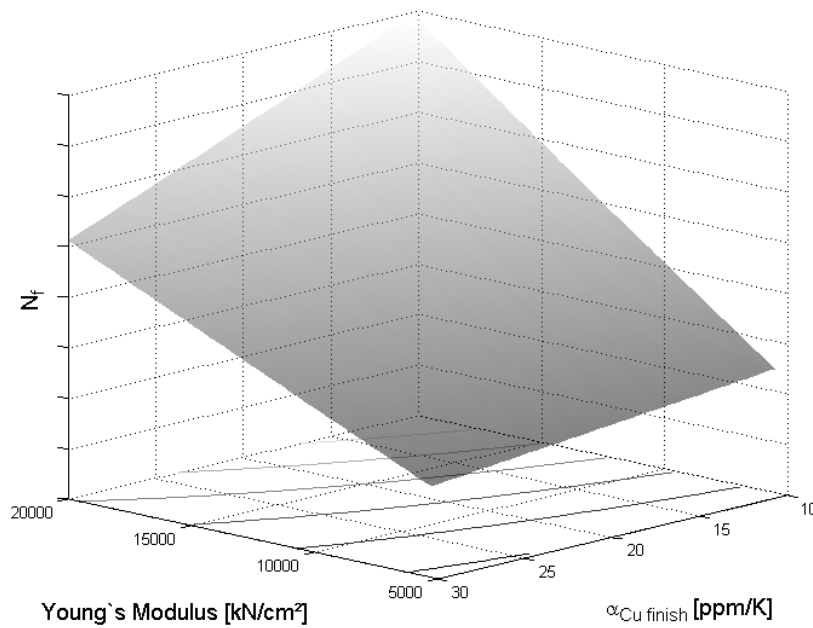


Figure 18: Number of stress cycles as function of $E_{Cu\ finish}$ and $\alpha_{Cu\ finish}$

It can be seen that the influence which arises from the Young's modulus prevails the influence of the coefficient of thermal expansion. That means Cu finishes with a high Young's modulus improve the thermo mechanical reliability of PCBs (see also chapter 3 'Comparison with "real" data').

Investigation of the influence of the drill hole diameter

To analyze the influence of the drill hole diameter d on the reliability of a PCB d has been varied between 100 μm and 750 μm .

An overview of the used parameters and their values shows table 4.

Table 4: Parameter used to analyse the influence of d on N_f

T_s	25 °C	D	20 %
T_f	150 °C	R_m	30 kN/cm ²
h	1.6 mm	$E_{Cu\ finish}$	-
d	300 μm – 750 μm	$\alpha_{Cu\ finish}$	-
$t_{PTH\ Cu}$	25 μm	T_g	135 °C
$t_{Cu\ finish}$	-	$E_{Epoxy}(T < T_g)$	848 kN/cm ²
$E_{el, PTH\ Cu}$	12400 kN/cm ²	$E_{Epoxy}(T > T_g)$	676 kN/cm ²
$E_{pl, PTH\ Cu}$	117 kN/cm ²	$\alpha_{Epoxy}(T < T_g)$	50 ppm/K
$\alpha_{PTH\ Cu}$	17 ppm/K	$\alpha_{Epoxy}(T > T_g)$	250 ppm/K
σ_y	25 kN/cm ²		

In figure 19 the effect of changing the drill hole diameter on the cycle capability of PCBs is shown. As can be seen with increasing diameter the number of cycles rise which also is verified by experimental data (see paragraph 3).

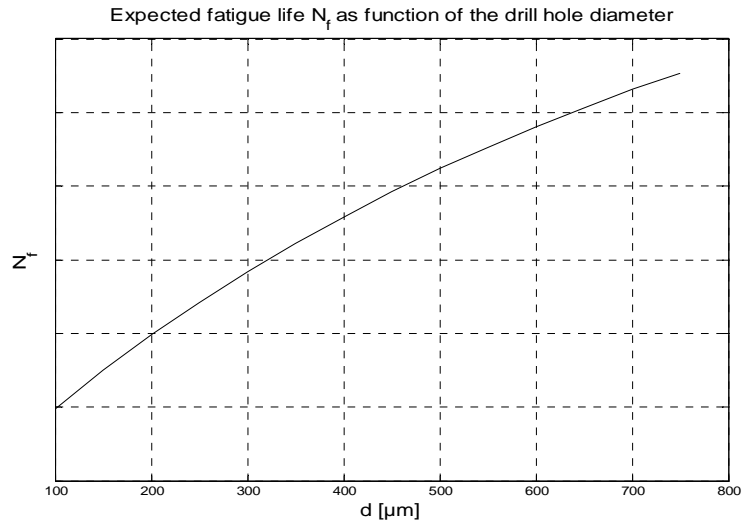


Figure 19: Number of stress cycles as function of d

Investigation of the influence of the PTH Cu thickness $t_{\text{PTH Cu}}$ and the coefficient of thermal expansion below T_g $\alpha_{\text{Epoxy}}(T < T_g)$

To analyze the influence of the PTH Cu thickness $t_{\text{PTH Cu}}$ and the coefficient of thermal expansion of the base material below the glass transition temperature $\alpha_{\text{Epoxy}}(T < T_g)$ on the reliability of a PCB $t_{\text{PTH Cu}}$ has been varied between 20 μm and 40 μm and $\alpha_{\text{Epoxy}}(T < T_g)$ has been varied between 40 ppm/K and 60 ppm/K.

An overview of the used parameters and their values shows table 5.

Table 5: Parameters used to analyze the influence of $t_{\text{PTH Cu}}$ and $\alpha_{\text{Epoxy}}(T < T_g)$ on N_f

T_s	25 °C	D	20 %
T_f	150 °C	R_m	30 kN/cm ²
h	1.6 mm	$E_{\text{Cu finish}}$	-
d	300 μm	$\alpha_{\text{Cu finish}}$	-
$t_{\text{PTH Cu}}$	20 μm – 40 μm	T_g	135 °C
$t_{\text{Cu finish}}$	-	$E_{\text{Epoxy}}(T < T_g)$	848 kN/cm ²
$E_{\text{el, PTH Cu}}$	12400 kN/cm ²	$E_{\text{Epoxy}}(T > T_g)$	676 kN/cm ²
$E_{\text{pl, PTH Cu}}$	117 kN/cm ²	$\alpha_{\text{Epoxy}}(T < T_g)$	40 ppm/K – 60 ppm/K
$\alpha_{\text{PTH Cu}}$	17 ppm/K	$\alpha_{\text{Epoxy}}(T > T_g)$	250 ppm/K
σ_y	25 kN/cm ²		

In figure 20 the effect of changing $t_{\text{PTH Cu}}$ and $\alpha_{\text{Epoxy}}(T < T_g)$ on the reliability of PCBs is displayed. The influence of $\alpha_{\text{Epoxy}}(T < T_g)$ on the cyclic capabilities of a PCB is significantly stronger than the influence of the PTH Cu thickness.

Expected fatigue life N_f as function of the PTH Cu thickness and $\alpha_{\text{Epoxy}}(T < T_g)$

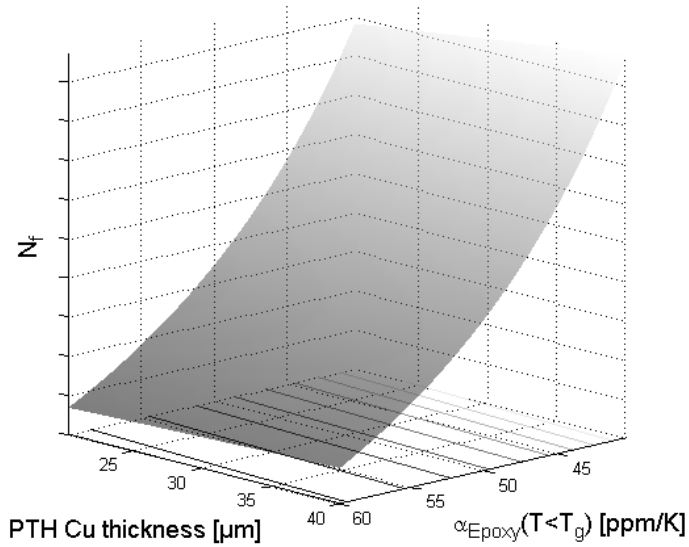


Figure 20: Number of stress cycles as function of $t_{\text{PTH Cu}}$ and $\alpha_{\text{Epoxy}}(T < T_g)$

3. Comparison with reliability data from practical investigations.

To validate the results of the modeling a comparison with measurement data is helpful. A test method to acquire test data in a relatively short time is the Interconnect Stress Test (IST) (~ 300 cycles / 24h). Provided that the achieved test cycles correlate with the fatigue life of the test samples the influence of several parameters on the cycle capability of PCBs can be studied.

To measure the influence of base material properties on the reliability of PCBs IST experiments with three different base materials keeping the PTH Cu properties constant were performed. The base materials differed in their glass transition temperatures T_g , their coefficient of thermal expansion below T_g $\alpha_{\text{Epoxy}}(T < T_g)$ and their coefficient of thermal expansion above T_g $\alpha_{\text{Epoxy}}(T > T_g)$ (see table 6).

Table 6: Base material properties

	T_g [°C]	$\alpha_{\text{Epoxy}}(T < T_g)$ [ppm/K]	$\alpha_{\text{Epoxy}}(T > T_g)$ [ppm/K]
Material A	138	61	276
Material B	144	57	255
Material C	170	42	200

The test parameters of each IST were

T_s = room temperature

T_f = 150°C

reject criterion = 10% warm resistance increase

Figure 21 displays the results of the IST experiments. As expected material A gives the worst result (\approx 370 cycles) followed by material B (\approx 1300 cycles) and with the best result material C (\approx 2900 cycles). The test of material C was aborted after 2932 cycles before reaching the reject criterion (no significant resistance increase; the IST system was needed for other tests) so the “expected” number of cycles probably is much higher than 3000 cycles.

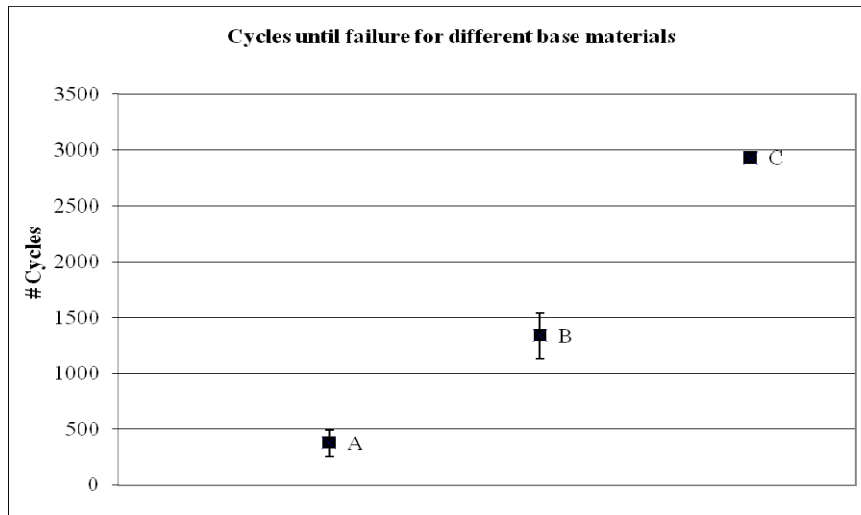


Figure 21: Results of IST experiments with different base materials A, B and C. The PTH Cu properties remained unchanged. For each base material six IST coupons were tested.

A comparison of figure 21 with figure 16 and 17 shows a good qualitative accordance of the experimental and theoretical results.

To test the influence of the PTH Cu finish on the reliability of PCBs IST experiments with three different Cu finishes (ENIG, HASL, chem. Sn) were carried out. During the tests all other PCB parameters (e.g. base material properties, Cu properties, drill hole diameter, PCB thickness, ...) were kept constant.

The test parameters of each IST were

T_s = room temperature

T_f = 150°C

reject criterion = 3% warm resistance increase or 1500 IST cycles passed

Unfortunately the thicknesses of the Cu finish layers differed among each other. The average thicknesses of the layers were as follows:

Table 7: Average thicknesses of the Cu finish layers

Finish	Thickness [µm]
ENIG	5.5
HASL	7.6
chem. Sn	2.3

Table 8 shows literature values for the Young's modulus and the coefficient of thermal expansion of the three Cu finish layers.

Table 8: Literature values for the Young's modulus and the coefficient of thermal expansion

Finish	Young's Modulus [kN/cm²]	Coefficient of Thermal Expansion [ppm/K]
ENIG	20000	13
HASL	3500	25
chem. Sn	5300	27

Figure 22 displays the results of the IST experiments. The material with the highest Young's modulus and the lowest coefficient of thermal expansion (ENIG) yields the best result: 1500 passed IST cycles with a resistance increase of ~ 1%. Due to its higher thickness HASL performed better than chem. Sn. Taking into account the influence of the more than three times higher thickness of the HASL layer it is

safe to say that chem. Sn has a more positive influence of the thermo mechanical reliability of PCBs than HASL which corresponds to the theoretical results of paragraph 2.3.

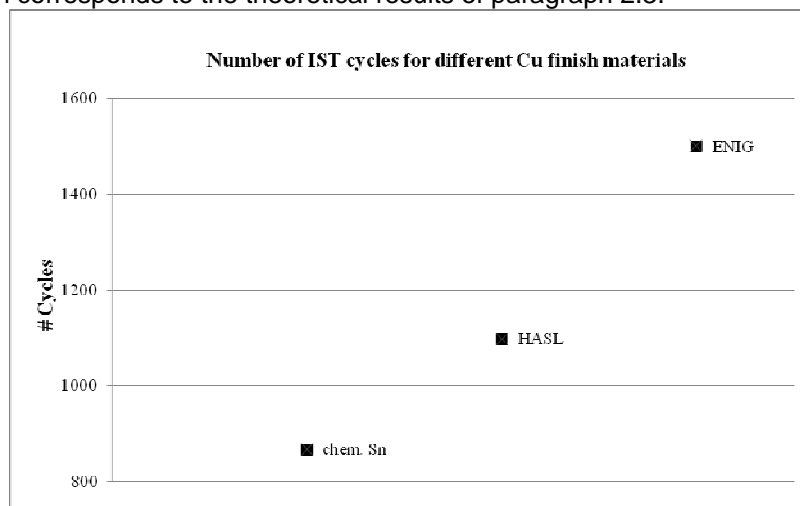


Figure 22: Results of IST experiments with different Cu finish materials ENIG, HASL and chem.Sn. The PTH Cu properties remained unchanged. For each Cu finish six IST coupons were tested.

Based on the results of several hundreds of IST investigations an analysis of the results in consideration of the drill hole diameter has been carried out. For comparable test coupons (similar thickness, similar base material properties, similar copper properties) the number of achieved IST cycles for drill hole diameters below 350 μm , for drill hole diameters between 350 μm and 650 μm and for drill hole diameters between 650 μm and 1000 μm were evaluated. The result is displayed in figure 23. With increasing drill hole diameter the number of IST cycles increases. The number of cycles seems to meet a saturation value (1000 cycles). This effect can be explained by the upper limit of test cycles of an IST which normally is set to 1000 cycles. Comparing figure 23 with figure 19 shows a good degree of conformity between model and experimental data.

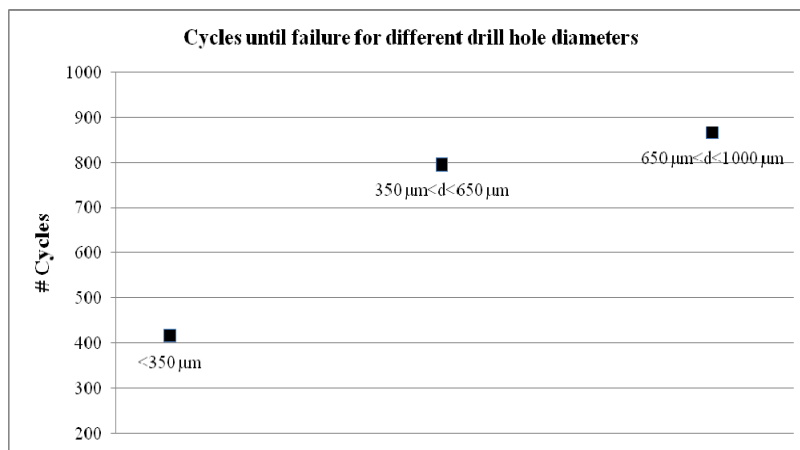


Figure 23: Number of achieved IST cycles against the drill hole diameter

4. Summary

Despite the amount of simplifying assumptions and approximations the model can be used to analyze qualitatively the influence of material properties and geometrical parameters on the thermo mechanical reliability of PCBs. Due to the degree of abstraction a knowledge of the (complex) behavior of the influencing variables is not needed. With this model only the general dependency of the thermo mechanical reliability of PCBs through holes on the influencing parameters can be described. Failure modes like corner cracks (e.g. due to the bending of annular rings) or failures like inner layer connection defects (ICDs) are not included. Nevertheless a comparison with experimental data shows good accordance between model and experiment.

A detailed in depth analysis of the cycle capability of a PTH including consideration of inhomogeneities (e.g non uniform temperature distribution; variation of the plating thicknesses), non-linearities (e.g. "smooth" glass transition), temperature and/or time dependency of state variables can not be made analytically. For this purpose numerical methods (e.g. FEA) have to be applied. Currently further work

is being carried out by one of the authors, Stefan Neumann to use numerical simulation of plated through holes to extend the scope of this investigation.

5. References

1. Werner Engelmaier, *Plated Through Hole Failures in Thermal Cycling: Analytical Considerations*, IPC-TR-579 (Round Robin Reliability Evaluation of Small Diameter Plated Through Holes in Printed Wiring Boards), 1988
2. Manson, S. S., *Thermal Stress and Low-Cycle Fatigue*, McGraw-Hill, New York, 1966
3. Steinberg, D. S., *PCB Plated Through Hole Thermal Stress Analysis*“, unpublished work, Boeing Aircraft Corporation, Seattle, Washington, October 1986